Axial orientation of molecular-beam-epitaxy-grown Fe3Si/Ge hybrid structures and its degradation

Maeda, Y; Jonishi, T; Narumi, K; Ando, YI; Ueda, K; Kumano, M; Sadoh, T; Miyao, M

APPLIED PHYSICS LETTERS **91**, 171910 (2007)

Axial orientation of molecular-beam-epitaxy-grown Fe_3Si/Ge hybrid structures and its degradation

Yoshihito Maeda[a] and Takafumi Jonishi
Department of Energy Science and Technology, Kyoto University, Sakyo-ku, Kyoto 606-8501, Japan

Kazumasa Narumi
Advanced Science Research Center, Japan Atomic Energy Agency, Takasaki 370-1292, Japan

Yu-ichiro Ando, Koji Ueda, Mamoru Kumano, Taizoh Sadoh, and Masanobu Miyao
Department of Electronics, Kyushu University, Motooka, Fukuoka 819-0395, Japan

(Received 21 August 2007; accepted 3 October 2007; published online 26 October 2007)

The axial orientation of molecular-beam-epitaxy (MBE)-grown $Fe_3Si(111)/Ge(111)$ hybrid structures was investigated by Rutherford backscattering spectroscopy. We confirmed that during MBE above 300 °C, the interdiffusion of Fe and Ge atoms results in a composition change and the epitaxial growth of FeGe in Fe_3Si. Low-temperature (<200 °C) MBE can realize fully ordered DO_3–Fe_3Si with highly axial orientation [minimum yield (χ_{min})=2.2%]. Postannealing above 400 °C results in a composition change and the degradation of axial orientation in the off-stoichiometric Fe_3Si. The significance of stoichiometry with regard to thermal stability and the interfacial quality of $Fe_3Si(111)/Ge(111)$ hybrid structures was also discussed. © *2007 American Institute of Physics*. [DOI: 10.1063/1.2801705]

Ordered DO_3–Fe_3Si has been attracting much attention as a highly spin-polarized ferromagnetic material that can be adapted to a few spin-injection devices.[1–3] Fe_3Si can be classified as a Heusler alloy and can be expected to have half-metallic properties and a high Curie temperature of 840 K, both of which are advantageous in enhancing spin-injection efficiency.[4–6] The molecular beam epitaxy (MBE) growth of Fe_3Si on GaAs can be successfully conducted[1] since the lattice constants of GaAs [a=0.5654 nm (Ref. 7)] and Fe_3Si [a=0.565 nm (Refs. 8 and 9)] are almost identical. Moreover, the epitaxial growth of Fe_3Si on Si (a=0.5431 nm), Ge [a=0.5658 nm (Ref. 7)], or SiGe substrates could further enhance its applicability to IV-group-based spin-electronic devices. The epitaxial growth on Si or Ge substrates has been investigated and certain interesting results indicating the strong dependence of this growth on the type of crystal plane were obtained.[2] In the case of both substrates, we have successfully accomplished high-quality MBE growth only on the (111) planes. The dominant factor influencing the epitaxial growth of Fe_3Si on Ge and Si has not yet been investigated in detail; however, we can infer that the differences in the nucleation and two-dimensional growth processes of each crystal plane may affect the quality of epitaxy.

In this study, we report the characterization of epitaxial single-crystal $Fe_3Si/Ge(111)$ hybrid structures synthesized by MBE and discuss the crucial factors for the realization of high-quality epitaxial growth on Ge(111) substrates.

Ferromagnetic Fe_3Si layers with off-stoichiometric ($Fe_{80}Si_{20}$) and stoichiometric ($Fe_{75}Si_{25}$) compositions, denoted by (4:1)- and (3:1)-Fe_3Si, respectively, were grown on 20-nm-thick Ge buffer layers grown epitaxially on Ge(111) substrates by employing a solid-source MBE process using Fe and Si coevaporation (deposition rates: 0.12–0.16 nm/s for Fe and 0.04 nm/s for Si).[2] The growth temperature (T_G) was controlled at 60–400 °C. Rutherford backscattering spectroscopy (RBS) using 2 MeV-$^4He^+$; random spectra for determining the depth profiles of the concentration and aligned spectra for evaluating the quality of the axial orientation of Fe_3Si along Ge⟨111⟩ were measured. The depth profiles of Fe and Ge atoms were deduced from the random spectra by using the layer model presented in the SIMNRA code.[10]

Figure 1 shows the Fe-channel random and aligned spectra along the Ge⟨111⟩ axis for each composition film, which were prepared at the T_G=200 and 300 °C, respectively. In this T_G range, we observed spectrum changes for both films.

Figures 2(a) and 2(b) show the changes in the Fe and Ge concentrations near the interface and χ_{min} as a function of

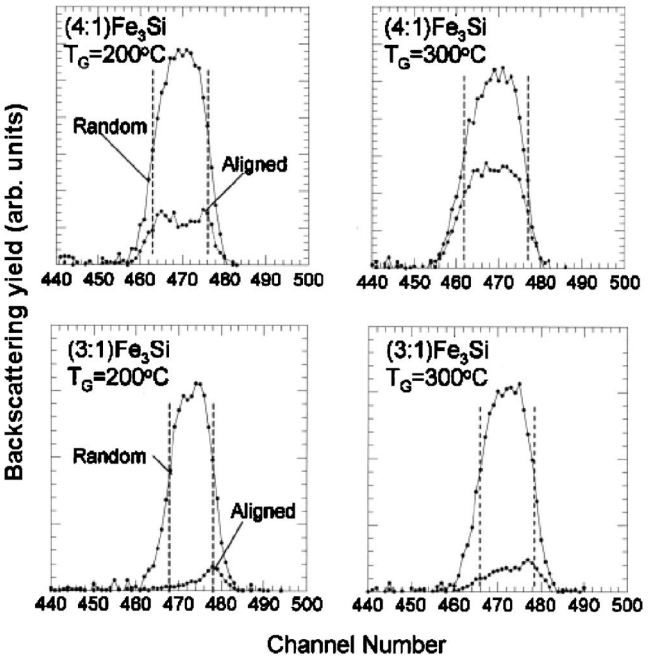

FIG. 1. Random and aligned RBS spectra of off-stoichiometric (4:1) and stoichiometric (3:1) compositions of Fe_3Si prepared at growth temperatures of 200 and 300 °C. The left and right dotted lines correspond to the Fe_3Si/Ge interface and Fe_3Si surface, respectively.

[a]Also at Advanced Science Research Center, Japan Atomic Energy Agency; electronic mail: ymaeda@zenon.energy.kyoto-u.ac.jp

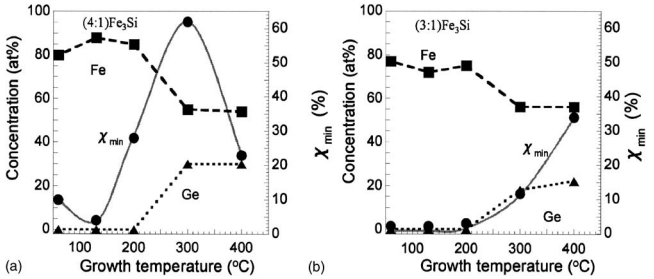

FIG. 2. Concentrations of the Fe and Ge atoms of the silicide layers at the interfaces and $\chi_{\min}$ as a function of growth temperature.

T_G, respectively. These indicate that high-quality epitaxial growth can be realized when $\chi_{\min}$ is smaller than 4% at 130 °C and below 200 °C for (4:1)- and (3:1)-Fe_3Si, respectively. In the case of stoichiometric (3:1)-Fe_3Si grown below 130 °C, we succeeded in realizing highly axial oriented crystal growth for the smallest $\chi_{\min}$ value (2.2%). However, with the increase in $\chi_{\min}$, the Fe concentration decreased and the Ge concentration increased above 200 or 300 °C. We found that this change in concentration due to the interdiffusion between Ge and Fe atoms at the interface strongly induces pronounced degradation in the epitaxial growth with the axial orientation of Fe_3Si.

These results reveal the following crucial factors for achieving high-quality epitaxial growth of Fe_3Si on Ge: First, the stoichiometry of Fe_3Si is a very important factor influencing layer growth. Second, the growth temperature should be lower than 130 °C. For the epitaxial growth of $Fe_3Si(100)/GaAs(001)$ hybrid structures, the optimal T_G range providing excellent crystalline and interfacial characteristics was reported to be $150\ °C < T_G < 250\ °C$. For higher T_G, the reactions of Fe and/or Si with Ga and/or As were similar to those observed during the epitaxial growth of Fe on GaAs.[1] The spin injection from Fe_3Si into GaAs at room temperature was carried out using a 35-nm-thick Fe_3Si layer grown on a *n*-GaAs layer at $T_G = 200\ °C$.[1] At a lower T_G (130 °C), higher quality epitaxial growth of $Fe_3Si(111)$ on Ge(111) can be realized, as compared to that on GaAs. The improvement in the quality of epitaxy with the decrease in the T_G can be attributed to the activity of Fe atomic diffusion during MBE growth.

Let us discuss the dependence of epitaxial growth on the stoichiometry of Fe_3Si. With regard to typical semiconductor epitaxy, the lattice mismatch between the grown films and substrates should be discussed first. The lattice constant of (4:1)-Fe_3Si at 300 K ($a = 0.5673$ nm) (Ref. 11) is slightly larger than that of (3:1)-Fe_3Si ($a = 0.5655$ nm).[8,12]

We can calculate the lattice mismatch ratio $\Delta(T)$ at a given temperature using $a = 0.5658$ nm at 300 K for Ge (Ref. 7) and their thermal expansion coefficients (α). For this calculation, we use the thermal expansion coefficient of $\alpha = 12.2 \times 10^{-6}/°C$ for bcc iron due to its uncertainty with regard to Fe_3Si. The $\Delta(T)$ values for (4:1)-Fe_3Si and (3:1)-Fe_3Si are +0.27% and −0.5% at 60 °C, +0.28% and −0.03% at 200 °C, and +0.30% and −0.02% at 300 °C, respectively. We observed a very small difference between the $\Delta(T)$ values of off-stoichiometric and stoichiometric Fe_3Si. It is unreasonable to hypothesize that such a small difference can lead to the pronounced degradation observed in the case of (4:1)-Fe_3Si grown above $T_G = 200\ °C$.

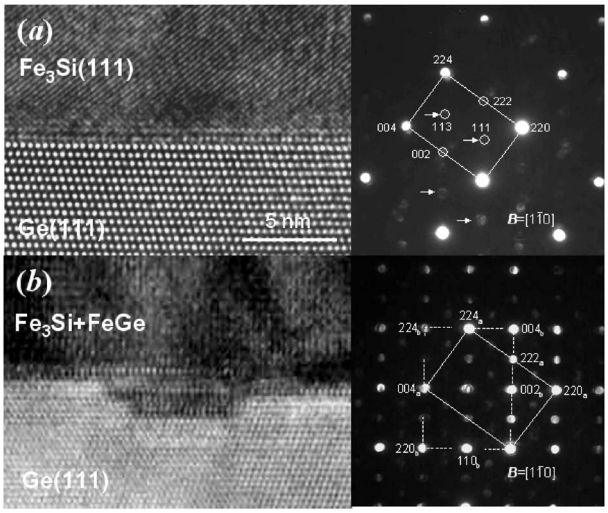

FIG. 3. High resolution transmittance electron microscopic images at interfaces of (4:1)-Fe_3Si grown at (a) 60 and (b) 400 °C, and the selected area electron diffraction (SAD) patterns for Fe_3Si. The key diagram for SAD (a) indicates ordered DO_3-Fe_3Si with superlattice diffraction from (111) and (113), which is indicated by the white arrows. The SAD pattern for (b) indicates the coexistence of cubic-FeGe epitaxially grown in $B2$-Fe_3Si.

Next, we focus our attention on the composition change due to atomic diffusion and on the formation of Fe–Ge compounds. Binary compounds, such as Fe_3Ge,[13] FeGe,[14] and $FeGe_2$,[15] may be formed by the diffusion of Ge atoms from the substrate during the MBE growth.

The growth layers formed at 60 and at 400 °C were investigated by transmittance electron microscopy (TEM) and selected area electron diffraction (SAD). Figure 3 shows the high resolution TEM images and SAD patterns. We confirmed that the atomically flat interface was formed at 60 °C; it suggests that no interdiffusion of Fe and Ge atoms through the interface occurred. On the other hand, in the case of growth at 400 °C, a very rough interface due to atomic interdiffusion was observed. The SAD pattern (zone axis$\|[1\bar{1}0]$) in Fig. 3(a) shows fundamental diffraction (220) and (004) spots for fcc lattice, (002) and (222) spots for ordered $B2$ structure, and superlattice reflection (111) and (113) spots for the ordered DO_3 structure of Fe_3Si. The analysis of the SAD pattern (b) of the two structures revealed that the superlattice spots (111) and (113) of the ordered DO_3 structure were lost, and that $B2$-Fe_3Si and cubic FeGe (c-FeGe) were assigned. From the concentration deduced from RBS, we can obtain the phase ratio of ($B2$-Fe_3Si):(c-FeGe)=1:3. The growth at 400 °C results in the increase in the Ge concentration of the Fe_3Si layer, thereby allowing c-FeGe to precipitate in the Fe_3Si layer. X-ray diffraction (XRD) also indicated the presence of c-FeGe with highly oriented crystallinity. The SAD pattern shown in Fig. 3(b) reveals the crystallographic relationships between $Fe_3Si(B2)$ and c-FeGe precipitates: c-FeGe(003)$\|$$Fe_3Si$(222) and c-FeGe$[1\bar{1}0]\|Fe_3Si[1\bar{1}0]$. The large lattice mismatch of $\Delta = -4.5\%$ for this epitaxy may be allowed partially. TEM observations (not shown) also revealed a clear phase separation between c-FeGe and $B2$-Fe_3Si. This results in lattice strain, which could be responsible for the degradation of the axial orientation of Fe_3Si. This hypothesis was also supported by the fact that $\chi_{\min}$ was 22% in Fig. 2(a).

In order to ensure the applicability of the Fe_3Si/Ge hybrid structure to certain spin-injection devices, we need

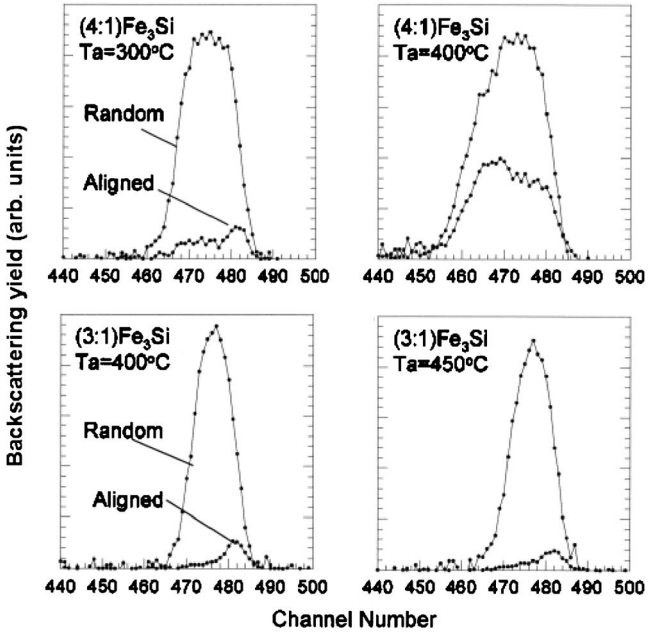

FIG. 4. Random and aligned RBS spectra of each composition $Fe_3Si(111)/Ge(111)$ hybrid structures annealed at 300–450 °C.

double or multiheterostructures such as $SiGe/Fe_3Si/Ge$ or $[Fe_3Si/Ge, Si, SiGe]_n$. We need to examine the thermal stability of Fe_3Si epitaxial layers already grown on Ge(111) and the interfacial structures before conducting MBE using Ge, Si, or SiGe on Fe_3Si layers. After postannealing high-quality samples with $\chi_{min}=2.2\%-4.0\%$ below the postannealing temperature $T_a=300$ °C, very few significant changes were observed in the interdiffusion and χ_{min} of the Fe_3Si layers.

Figure 4 shows the random and aligned spectra of RBS after annealing above $T_a=300$ °C. Only in the (4:1)-Fe_3Si layer annealed at $T_a=400$ °C for 2 h, a pronounced increase in the aligned yield, corresponding to the increase in χ_{min}, and an increase in the width of the random RBS spectrum were observed.

Figures 5(a) and 5(b) show the concentration of the Fe_3Si layer and χ_{min} as a function of T_a, respectively. Moreover, in this case, we found that there exists a very clear correlation between the concentration change due to interdiffusion near the interface and the increase in χ_{min} (degradation of axial orientation), and that the thermal stability behaviors of the Fe_3Si layers of both the compositions differ significantly. The stoichiometric Fe_3Si layers are more thermally stable than the off-stoichiometric one. The (4:1) sample annealed at $T_a=400$ °C was no longer a single crystal Fe_3Si and the formation of c-FeGe was also confirmed by XRD. In contrast, the (3:1) sample maintained its ordered

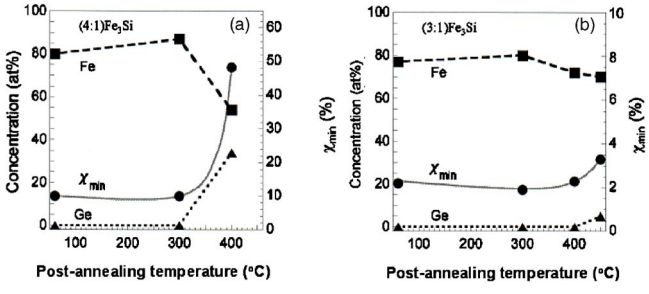

FIG. 5. Concentrations of the Fe and Ge atoms of the silicide layers at the interfaces and χ_{min} as a function of postannealing temperature. The annealing time was 2 h.

DO_3 structures and crystallinity with good axial orientation even after being postannealed at 450 °C for 2 h, as shown in Fig. 5(b). Based on the results of the postannealing experiment shown in Figs. 4 and 5, it can be inferred that the MBE growth of some of the semiconductor layers on Fe_3Si epitaxial layers can be performed at least up to 300 °C for the (4:1) sample and up to 400 °C for the (3:1) one.

We can conclude that the T_G should be lower than 130 °C under the present deposition rates. It should be emphasized that the stoichiometry of Fe_3Si layers is very important to realize highly axial orientation and improved thermal stability of the ordered structure. The thermal stability observed in this study might be related to the diffusion activity of Fe atoms in Fe_3Si. It has been reported that in Fe-rich DO_3-Fe_3Si bulk crystals, the excess Fe atoms can diffuse into the Si lattice site.[16] If this scheme is applied to the Fe_3Si layers in MBE growth, the Fe atoms at the Si site might be sufficiently unstable to diffuse actively into the Ge substrate. Hertfort *et al.*[17] investigated electrical conduction of $Fe_{3-x}Si_{1+x}$ and reported the distinct minimum resistivity due to structural ordering around stoichiometric Fe_3Si and the significant increase due to disordering in the off-stoichiometric compositions. This result is important in considering the relationship between stoichiometry and structural ordering, which might be affected by the Fe atom diffusion. However, in order to discuss this further, we need to conduct a detailed investigation on the activity of Fe or Ge atomic diffusion near the growing interface during MBE.

This study was supported by a Grant-in-Aid for Scientific Research on Priority Area No. 18063018 and the Grant No. 17360011 from the MEXT in Japan.

[1] A. Kawaharazuka, M. Ramsteiner, J. Herfort, H.-P. Schenherr, H. Kostial, and K. H. Ploog, Appl. Phys. Lett. **85**, 3492 (2004); J. Herfort, H.-P. Schoenherr, and K. H. Ploog, *ibid.* **83**, 3912 (2003).
[2] T. Sadoh, M. Kumano, R. Kizuka, K. Ueda, A. Kenjo, and M. Miyao, Appl. Phys. Lett. **89**, 182511 (2006).
[3] T. Yoshitake, D. Nakagauchi, T. Ogawa, M. Itakura, N. Kuwano, Y. Tomokiyo, T. Kajiwara, and K. Nagayama, Appl. Phys. Lett. **86**, 26250 (2005).
[4] R. A. de Groot, F. M. Mueller, P. C. van Engen, and K. H. Buschow, Phys. Rev. Lett. **50**, 2024 (1983).
[5] M. J Otto, H. Feil, R. A. van Bruggen, and C. Haas, J. Magn. Magn. Mater. **70**, 33 (1987).
[6] S. Fujii, S. Sugimura, S. Ishida, and S. Asano, J. Phys.: Condens. Matter **43**, 8583 (1990).
[7] *Semiconductors: Data Handbook*, 3rd ed., edited by O. Madelung (Springer, Berlin, 2003), p. 45.
[8] *Persons Handbook of Crystallographic Data for Intermetallic Phases*, 2nd ed., edited by P. Villars and L. D. Calvart (ASM International, Materials Park, OH, 1991), Vol. 3, p. 515.
[9] K. G. Nath, F. Maeda, S. Suzuki, and Y. Watanabe, J. Appl. Phys. **90**, 1222 (2001).
[10] M. Mayer, AIP Conf. Proc. **475**, 541 (1999).
[11] F. Richter and W. Pepperhoff, Arch. Eisenhuettenwes. **45**, 107 (1974).
[12] S. N. Mishra, D. Rambabu, A. K. Grover, R. G. Pillay, P. N. Tandon, H. G. Devare, and R. Vijayaraghavan, J. Appl. Phys. **57**, 3258 (1985); M. Singh and S. Bhan, Cryst. Res. Technol. **19**, K81 (1984).
[13] R. Sobczak, Monatsch. Chem. **106**, 1389 (1975); A. K. Blom, O. Beckman, and M. Richardson, Solid State Commun. **5**, 977 (1967).
[14] B. Lebech, J. Bernhard, and T. Freltoft, J. Phys.: Condens. Matter **1**, 6105 (1989).
[15] H. J. Wallbaum, Z. Metallkd. **35**, 218 (1973).
[16] W. A. Hines, A. H. Menotti, J. I. Budnick, T. Litrenta, V. Niculescu, and K. Raj, Phys. Rev. B **13**, 4060 (1976).
[17] J. Hertford, H.-P. Schoenherr, K.-J. Friedland, and K. H. Ploog, J. Vac. Sci. Technol. B **22**, 2073 (2004).